International Journal of Geo-Information

MDPI

Article

The Spatial Equilibrium Model of Elderly Care Facilities with High Spatiotemporal Sensitivity and Its Economic Associations Study

Hongyan Li, Rui Li *, Jing Cai and Shunli Wang

State Key Laboratory of Information Engineering in Surveying, Mapping and Remote Sensing, Wuhan University, 129 Luoyu Road, Wuhan 430079, China; hong_yan_li@whu.edu.cn (H.L.); jingcai@whu.edu.cn (J.C.); shunliwang@whu.edu.cn (S.W.)

* Correspondence: ruili@whu.edu.cn; Tel.: +86-027-68778247

Abstract: The global population aging poses new challenges in allocating care facilities for the elderly. This demographic trend also influences economic development and the quality of urban life. However, current research focuses on the supply of elderly care facilities and primarily uses administrative divisions as a scale, resulting in low spatiotemporal sensitivity in evaluating the spatial equilibrium of elderly care facilities (SEECF). The relationship between the SEECF and economic development is not clear. In response to these problems, we proposed a spatial equilibrium model of elderly care facilities with high spatiotemporal sensitivity (SEM-HSTS) and explored the spatiotemporal associations between the SEECF and economic development. Considering the spatial accessibility rate of elderly care services (SARecs) and the spatiotemporal supply–demand ratio for elderly care services (STSDRecs), two types of supply–demand relationship factors were constructed. Then, a spatiotemporal accessibility of medical services (STAms) factor was obtained based on a modified two-step floating catchment area (M2SFCA) method. On this basis, the SEM-HSTS was constructed based on the theory of coordinated development. Further, a panel threshold model was employed to evaluate the influence relationships among population aging, SEECF, and gross domestic product (GDP) in different phases. Finally, spatial autocorrelation and Geodetector explored the spatial associations between SEECF and GDP across complex urban land use categories (ULUC). The experimental results at a 100-m grid scale showed that the SEM-HSTS exhibited higher spatiotemporal heterogeneity than the classical accessibility method, with elevated spatiotemporal sensitivity. Effectively identified various spatial imbalances, such as undersupply and resource waste. The panel model captured phased relationship changes, showing that SEECF had inhibitory and promotional effects on GDP in pre- and post-aging societies, with stronger effects as balance approached. Moreover, the combined interaction of ULUC and GDP had a more significant influence on SEECF than any individual factor, with GDP exerting a more significant influence. This study provides an empirical basis for creating resource-efficient elderly care facility systems and optimizing layouts.

Keywords: population aging; spatial equilibrium; spatiotemporal sensitivity; GDP; spatial associations

Citation: Li, H.; Li, R.; Cai, J.; Wang, S. The Spatial Equilibrium Model of Elderly Care Facilities with High Spatiotemporal Sensitivity and Its Economic Associations Study. *ISPRS Int. J. Geo-Inf.* **2024**, *13*, 268. https://doi.org/10.3390/10.3390/ijgi13080268

Academic Editor: Wolfgang Kainz

Received: 25 April 2024
Revised: 17 July 2024
Accepted: 24 July 2024
Published: 27 July 2024

1. Introduction

According to the aging classification standards established by the United Nations in 1956 [1], when the proportion of individuals aged 65 and above exceeds 7% in a country or region, it signifies the transition into an aging society; surpassing 14% indicates a deeply aged society; and crossing the threshold of 20% denotes entry into a super-aged society. According to reports from the United Nations, the global population is entering an aging phase, with the number and proportion of elderly populations increasing in almost every country. Population aging may emerge as one of the most significant social trends of the 21st century. However, as the degree of aging deepens, the supply of elderly care services fails to meet the increasing demands of the elderly population. Issues such as the lack of

comprehensive planning and the irrational spatial allocation of elderly care facilities are becoming increasingly prominent [2–6]. Therefore, addressing population aging trends effectively and optimizing the layout of elderly care facilities to promote supply–demand balance holds paramount significance.

Spatial equilibrium has long been considered a cornerstone in the planning research of elderly care facilities [7–10]. The spatial equilibrium of elderly care facilities (SEECF) implies that the optimal state is one where the supply of elderly resources within a specific spatial range matches the demands of the elderly population. Any spatial imbalances resulting from supply–demand disparities can be rectified by restructuring spatial arrangements and optimizing existing spaces [11]. Current research on the SEECF varies in terms of the types of elderly care facilities, research methods, and spatial scale. Firstly, many studies focus solely on service-oriented facilities catering to the daily living, care, and recreational needs of the elderly population. Neglecting the essential medical and nursing care facilities required for the elderly daily life [12–17]. Secondly, in terms of research methodologies, there is a tendency to downplay the actual needs of the elderly population in favor of emphasizing the supply of elderly care facilities. As seen in methods such as kernel density estimation [18–20], service coverage rates [21], the Huff model [22–25], and accessibility assessments [26–33]. Additionally, in terms of scale, precise population data are fundamental components of effective urban management and strategic planning [34–36]. However, many existing studies utilize administrative divisions, such as districts [16,37–39], streets [40–43], or communities [38,44–46], to represent population centers. This leads to less accurate simulations of real-world scenarios. The deficiencies in different types of research have brought severe challenges to the spatiotemporal sensitivity measurement of regional SEECF, making it difficult to conduct a refined study of the SEECF. The refined analysis of the SEECF is the basis for providing a decision-making basis for the scientific planning and management of elderly care facilities [47,48]. It is necessary to propose a fine-scale spatial equilibrium model of elderly care facilities that takes into account the types of elderly care facilities and the relationship between supply and demand.

Population aging plays a significant role in the transition of China's economic growth. That is from the previous emphasis on the gross domestic product (GDP) scale expansion to a shift towards high-quality economic development. There is a wealth of research on the relationship between population aging and economic development [49,50]. Conflicting conclusions exist concerning internal mechanisms and consequences due to varying research perspectives. Some studies [51–54] find a significant negative impact of population aging on economic growth. In contrast, others [55–57] argue that population aging may contribute to GDP growth. Additionally, some research [58] suggests that with population aging, the GDP growth rate initially increases before decreasing. Moreover, existing studies on the relationship between elderly population factors and economic growth rarely integrate different attributes of the elderly population into the same research framework. Most studies only explore quantitative correlations, with limited research on spatial associations. Furthermore, the relationships among population aging, SEECF, and economic development remain unclear. Therefore, based on the panel threshold model, this study considers that population factors and facility allocation equilibrium simultaneously affect economic development. Thus, studying their influence patterns to provide multi-dimensional references for facility planning and sustainable economic development. While there is extensive research on the relationship between GDP and urban land use categories (ULUC) [59–67], much of it focuses solely on construction land type [68–71]. Hence, this study further explores the spatial associations between the SEECF, GDP, and ULUC.

At present, research on the spatial equilibrium model of elderly care facilities is limited to service-type elderly care facilities. In the process of model construction, the focus is on the supply capacity of elderly care facilities, and the actual needs of the elderly population are weakened. The spatial scale of the research is mostly based on administrative divisions. This large-scale regional setting makes the spatial equilibrium evaluation of elderly care facilities low in spatiotemporal sensitivity. Most of the research on the SEECF and economic

development has only explored the relationship between numerical distribution and rarely involved the analysis of spatial association relationships. At the same time, the impact of ULUC on the SEECF has not been considered. Therefore, it is urgent to construct a fine-scale spatial equilibrium model of elderly care facilities that takes into account different types of elderly care facilities and supply–demand relationships and further quantitatively analyze its spatial association with economic development and ULUC.

To solve the above problems, this study first took into account different types of elderly care facilities, such as service-oriented and medical care-oriented, and considered the supply capacity of elderly care facilities and the actual needs of the elderly population to construct a spatial equilibrium model of elderly care facilities with high spatiotemporal sensitivity (SEM-HSTS). At the 100-m fine grid scale, considering the supply capacity of elderly care facilities and the actual needs of the elderly population, we proposed constructing two factors, i.e., the spatial accessibility rate of elderly care services (SARecs) and the spatiotemporal supply–demand ratio for elderly care services (STSDRecs). By employing the modified two-step floating catchment area (M2SFCA), we obtained the spatiotemporal availability of medical services (STAms) factor. Facing the needs of per capita resource fairness and facility accessibility efficiency, the coordination degree model was introduced to calculate the SEECF with high spatiotemporal sensitivity. On this basis, considering the high spatiotemporal sensitivity of the SEM-HSTS, this study further explored its comprehensive association with economic development. Considering that the elderly population factor and the SEECF will have an impact on GDP at the same time, we investigated the phased influence relationships among the population aging, SEECF, and GDP based on the threshold effect test. Through bivariate local spatial autocorrelation analysis and risk factor detection, we quantitatively analyzed the spatial associations among SEECF, GDP, and ULUC. This study can provide valuable insights into the precise planning and layout of elderly care facilities and furnish a scientific theoretical basis for the multi-dimensional management of such facilities within the context of joint economic development and urban spatial structure.

2. Methods

Achieving spatial balance in elderly care facilities necessitates a comprehensive matching between the quantity and quality of elderly care service resources and the demands of the elderly population. Elderly individuals exhibit a high sensitivity to travel distance, with inconvenience and distance being primary factors affecting their access to elderly care services and medical services. The spatial equilibrium of elderly care facilities (SEECF) is an index to quantify the balance of supply and demand distribution of elderly care facilities. Accordingly, this study proposed the construction of three factors at a 100-m grid scale, i.e., SARecs, STSDRecs, and STAms. These factors were integrated with a coordination degree model to calculate the SEECF. By comparing the SEECF with accessibility using three indicators—standard deviation, q-value of Geodetector, and the number of significant regions of local spatial autocorrelation—this study established SEM-HSTS. Secondly, leveraging the advantages of high temporal sensitivity, we employed a panel threshold model to investigate the phased influence of SEECF on economic development in the context of population aging. Lastly, based on the characteristics of high spatial sensitivity of SEM-HSTS and Geodetector, we analyzed the spatial associations between the SEECF and economic development under different ULUC, thereby obtaining precise spatiotemporal associations of the SEECF and economic development. The overall technical process is illustrated in Figure 1. It is divided into two main components, i.e., study of the SEM-HSTS and study of the associations between the SEECF and economic development.

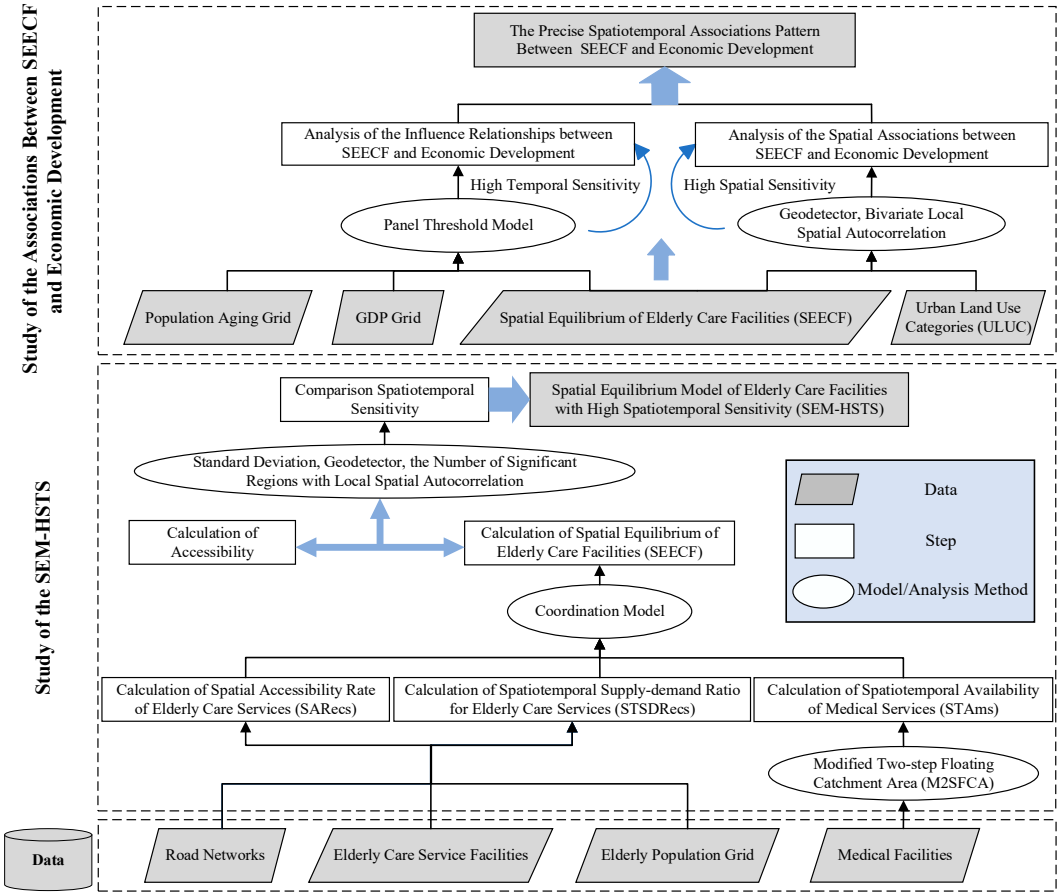

Figure 1. Technology roadmap.

2.1. Study of the SEM-HSTS

2.1.1. Spatial Accessibility Rate of Elderly Care Services (SARecs)

The network analysis method can be used to analyze service coverage based on the existing road network system, which, compared to directly selecting straight-line distance as the service radius, can more accurately reflect the actual service range of elderly care facility points. The specific steps for constructing the SARecs were as follows: (1) Set the walking speed v of the elderly, calculate the time consumed for walking based on the road length, add the walking time cost attribute as the time impedance attribute, and construct a topologically connected central urban road traffic network. (2) Based on the created road network dataset, construct service areas using network analysis tools, load the locations of elderly care service facilities, set n interruption values of time impedance $t_1, t_2, \ldots t_n$, and determine the service range of elderly care facilities in each period. (3) Score the service areas for each period as $\varepsilon_1, \varepsilon_2, \ldots \varepsilon_n$. To enhance the rationality of the factor from the demand perspective, for regions with an aging degree α greater than the aging society standard α_0, the scores needed to be multiplied by the loss function ω [18]. The scores remain unchanged for other regions, resulting in the final SARecs (θ), calculated as follows.

$$\varepsilon(t) = \begin{cases} \varepsilon_1, 0 < t \leq t_1 \\ \vdots \\ \varepsilon_n, t_{n-1} < t \leq t_n \end{cases} \tag{1}$$

$$\omega = e^{-\alpha} \tag{2}$$

$$\theta(x_i, y_i) = \begin{cases} \varepsilon(t), & \alpha \leq \alpha_0 \\ \varepsilon(t) \cdot \omega, & \alpha > \alpha_0 \end{cases} \tag{3}$$

In Equation (1), $\varepsilon(t)$ represents the service capacity score of elderly care service facilities in different periods $t_1, t_2, \ldots t_n$. Equation (2) defines the loss function ω, where α signifies the degree of population aging. Equation (3) introduces $\theta(x_i, y_i)$ as the SARecs at location (x_i, y_i), with α_0 denoting the standard of an aging society, namely 7% [1]. Elderly care service facilities of different scales exhibit a common phenomenon of service capacity attenuation. That is, as the distance from the facilities increases (represented by time t), their service capacity diminishes (represented by the service capacity score $\varepsilon(t)$). Compared to methods such as kernel density, SARecs reveals greater spatial heterogeneity, indicating higher spatial sensitivity.

2.1.2. Spatiotemporal Supply–Demand Ratio for Elderly Care Services (STSDRecs)

The supply–demand ratio reflected the degree of alignment between the demand of elderly populations and the supply of elderly care service facilities at different spatial locations, simultaneously capturing facilities' quantity and occupancy status. In contrast to the service coverage rate, it avoided the misconception of resource wastage due to proximity in layout. With the elderly population as the focus, if they fell within the service radius of elderly care service facilities, they could access the services provided by these facilities. Different scales of elderly care service facilities had different service radii, reflecting spatial heterogeneity. Additionally, the service capacity (number of beds) of elderly care service facilities and the elderly population varied over time, demonstrating temporal heterogeneity. In essence, it exhibited high spatiotemporal sensitivity. The formula for calculating the STSDRecs is as follows:

$$\zeta(x_i, y_i)_T = \frac{\sum_m b_{m,r,T}}{apop_T} \tag{4}$$

In Equation (4), $\zeta(x_i, y_i)_T$ denotes the STSDRecs at location (x_i, y_i) and time T while $apop_T$ represents the elderly population counts at location (x_i, y_i) and time T. Here, m stands for the number of facilities within the service radius of the elderly care service facility from position (x_i, y_i), and $b_{m,r,T}$ signifies the average supply of beds within the radius r of elderly care service facilities at time T. The service radius is calculated based on road network distance rather than Euclidean distance.

2.1.3. Spatiotemporal Availability of Medical Services (STAms)

In medical travel, proximity and convenience are the primary attractions. The Modified Two-Step Floating Catchment Area (M2SFCA) method [72] assessed the availability of medical facility resources per capita. Considering that not all facility resources are fully utilized in the real world, an additional distance decay function was introduced in the numerator to relax the original model assumptions, allowing for an inevitable loss in the weighted sum of demand compared to the total supply, thus making the model more realistic. As medical facility supply (number of beds) and elderly population demand (number of elderly populations) change over time, considering the distance decay effect, it exhibited high spatiotemporal sensitivity. This study calculated the STAms based on the road network, with the formulas as follows [72]:

$$R_{j,T} = \frac{S_{j,T}}{\sum_{k \in (d_{kj} \le d_0)} G(d_{kj}, d_0) D_{k,T}} \tag{5}$$

$$G(d_{kj}, d_0) = \begin{cases} \frac{e^{-(\frac{1}{2})\cdot(\frac{d_{kj}}{d_0})^2} - e^{-(\frac{1}{2})}}{1 - e^{-(\frac{1}{2})}}, & d_{kj} \le d_0 \\ 0, & d_{kj} > d_0 \end{cases} \tag{6}$$

$$A^F_{i,T} = \sum_{j \in (d_{ij} \le d_0)} R_{j,T} G(d_{ij}, d_0) = \sum_{j \in (d_{ij} \le d_0)} \left\{ \frac{S_{j,T}}{\sum_{k \in (d_{kj} \le d_0)} G(d_{kj}, d_0) D_{k,T}} \right\} G(d_{ij}, d_0) \tag{7}$$

In Equation (5), where j represents primary healthcare facilities, k denotes grid points of the elderly population, d_0 stands for distance threshold, d_{kj} signifies the distance between primary healthcare facility j and elderly population grid point k, $D_{k,T}$ represents the elderly population counts at grid point k and time T, and $S_{j,T}$ represents the total supply scale at primary healthcare facility j and time T, precisely the number of beds. For primary healthcare facilities without designated beds or experiencing data deficiencies, virtual bed counts are calculated based on the proportional relationship between bed counts and the number of physicians and nurses. $R_{j,T}$ denotes the weighted sum ratio of the total supply scale to the demand scale at the primary healthcare facility j and time T, i.e., the supply–demand ratio. $G\left(d_{kj}, d_0\right)$ represents the Gaussian distance decay model with its specific calculation formula provided in Equation (6). For each grid point i, primary healthcare facilities j are searched within a radius of d_0, and the sum of all supply rates $R_{j,T}$ is obtained to yield the STAms at the elderly population grid point i and time T, denoted as $A_{i,T}^{F}$ (Equation (7)).

2.1.4. Spatial Equilibrium Model of Elderly Care Facilities with High Spatiotemporal Sensitivity (SEM-HSTS)

The theory of coordinated development emphasizes the harmony and coordination among elements within a system, which can propel comprehensive advancement and enhance overall efficiency and level [73]. In constructing spatial equilibrium models, considerations were given to the fact that the elderly population prioritizes daily service needs over medical requirements. Consequently, two factors were proposed for elderly care service facilities, i.e., SARecs and STSDRecs, while STAms was designated for medical facilities. Both categories of facility indicators catered to fairness and efficiency requirements. Fairness ensured that residents in each region could access essential elderly care services, with minimal per capita resource allocation disparity manifested in the supply–demand ratio within STSDRecs and STAms factors. Efficiency involved facilitating residents' efficient and convenient access to elderly care facilities and maximizing the utilization of eldercare resources, demonstrated through SARecs and the Gaussian distance decay function within the STAms factor. This significantly enhanced the method's rationality, scientific nature, and goal orientation. Additionally, due to the advantages of the three types of factors in terms of spatiotemporal sensitivity, the resulting SEM-HSTS also exhibited high spatiotemporal sensitivity. The specific calculation formulas are provided below [73].

$$D_T = \sqrt{C_T \times E_T} \tag{8}$$

$$C_T = \left[\frac{\prod_{l=1}^{u} \delta_{l,T}}{\left(\frac{1}{u}\sum_{l=1}^{u} \delta_{l,T}\right)^{u}} \right]^{\frac{1}{u}} \tag{9}$$

$$E_T = \sum_{l=1}^{u} a_{l,T}\delta_{l,T} \tag{10}$$

In the equations, D_T, C_T, and E_T represent SEECF, coordination, and comprehensive evaluation indicators at time T, respectively. $\delta_{l,T}$ denotes the Gini coefficient for the l-th indicator of the system at time T, corresponding to the three factors—SARecs, STSDRecs, and STAms. The weight $a_{l,T}$ for the l-th indicator at time T is determined using the Analytic Hierarchy Process, satisfying $\sum_{l=1}^{u} a_{l,T} = 1$, where u is the number of indicators. It is important to note that the Gini coefficient is calculated based on Voronoi polygon regions, which are generated from elderly care facility points, and spatial interpolation is performed to obtain the grid-scale SEECF.

2.2. Study of the Associations between SEECF and Economic Development

2.2.1. Influence Analysis between SEECF and GDP Based on the Panel Threshold Model

The rational allocation of elderly care facilities is crucial in enhancing urban quality, achieving social equity, and fostering economic development. However, there has been a lack of research that analyzes the interrelationships among population aging, SEECF, and economic development within the same framework. In the following sections, leveraging the advantages of the high temporal sensitivity of SEM-HSTS and the enhanced significance of endogenous threshold effects in panel threshold models, along with improved accuracy in estimating threshold values, we integrated population aging, SEECF, and GDP into a unified research framework to identify their phased relationship patterns. We established the model as follows [49]:

$$Y_{iT} = \beta_1 aging_{iT} \cdot I(D_{iT} < \gamma_1) + \beta_2 aging_{iT} \cdot I(\gamma_1 \le D_{iT} < \gamma_2) + \cdots + \beta_n aging_{iT} \cdot I(D_{iT} \ge \gamma_n) + \rho X_{iT} + \varepsilon_{iT} \quad (11)$$

$$Y_{iT} = \beta_1 D_{iT} \cdot I(aging_{iT} < \gamma_1) + \beta_2 D_{iT} \cdot I(\gamma_1 \le aging_{iT} < \gamma_2) + \cdots + \beta_n D_{iT} \cdot I(aging_{iT} \ge \gamma_n) + \rho X_{iT} + \varepsilon_{iT} \quad (12)$$

In the equations, $I(\cdot)$ denotes a threshold function taking values of 1 or 0, where it evaluates to 1 if the condition inside the parentheses is met and 0 otherwise. The variables inside the parentheses represent threshold variables, with $\gamma_1, \gamma_2 \ldots \gamma_n$ representing threshold values; Y_{iT} denotes GDP; $\beta_1, \beta_2 \ldots \beta_n$ represent the degrees of the influence of core variables on GDP at different threshold levels; ρ denotes the parameter capturing the influence of control variables; X_{iT} represents control variables; and ε_{iT} is independently and identically distributed residuals. This study focuses on the relationships among population aging ($aging_{iT}$), SEECF (D_{iT}), and GDP. Equation (11) examines the influence of population aging on GDP with D_{iT} as the threshold variable. At the same time, Equation (12) investigates the influence of D_{iT} on GDP with population aging as the threshold variable. The residual sum of squares is computed for Equations (11) and (12) to calculate threshold values, followed by calculating the F-statistic to test the significance of the threshold effects. The null hypothesis for the threshold effects model is as follows [49]:

$$H_0 : \beta_1 = \beta_2 = \cdots = \beta_n \quad (13)$$

If the test for threshold effects does not reject the null hypothesis, it indicates the absence of threshold effects. Conversely, rejecting the null hypothesis suggests the presence of threshold effects. Subsequently, a test is conducted on the threshold values by constructing the Likelihood Ratio (LR) statistic to examine their significance. LR is the ratio of the value of the likelihood function of the unconstrained model to the value of the likelihood function of the constrained model. The asymptotic distribution of the LR statistic depends on sample moments and cannot be directly obtained. Therefore, the Bootstrap method obtains the asymptotic distribution to derive the corresponding p-value. Upon confirming the presence of threshold effects, the confidence interval for the threshold values is further determined [49]. Building on these model specifications and hypothesis tests, empirical tests are conducted on the relationships among the variables of interest in this study.

The selection of variables in the model is shown in Table 1 below, and logarithmic transformations are applied to GDP, population size, and road network length to mitigate endogeneity and multicollinearity.

Table 1. Variable selection in the panel threshold model.

Variable Type	Variable Name
Dependent variable	GDP
Core explanatory variables	SEECF; population aging
Control variables	Population size; road network length

2.2.2. Spatial Associations Analysis between SEECF and GDP Based on the Bivariate Local Spatial Autocorrelation

To obtain comprehensive associations between the SEECF and economic development, it was essential to analyze the causal relationships between variables and explore their spatial associations. This study began by utilizing the bivariate spatial autocorrelation, which is highly applicable and effective in describing the spatial association and dependence characteristics between two geographic elements. The Bivariate Moran's I statistic was employed to explore the spatial association features between the SEECF and GDP. The principle is outlined as follows:

$$I_i^B = cD_i \sum_h \omega_{ih} GDP_h \tag{14}$$

In Equation (14), D_i represents the SEECF at grid i; GDP_h denotes the GDP value at grid h, where grid h is spatially adjacent to grid i; c denotes a constant proportion factor; ω_{ih} represents the spatial weight matrix; and I_i^B indicates the local spatial distribution correlation between the SEECF at grid i and GDP at grid h. The results can be classified into the following four types of spatial clusters: H-H (high-high), L-L (low-low), H-L (high-low), and L-H (low-high).

2.2.3. Spatial Associations Analysis among SEECF, GDP, and ULUC Based on Geodetector

The analysis of the spatial association between the SEECF and GDP, based on bivariate local spatial autocorrelation, only examined the degree of clustering association. However, ULUC also played a significant role in the spatial association analysis of both variables. The high spatial sensitivity of the SEM-HSTS provided an excellent prerequisite for studying spatial associations under different ULUC. Geodetector, a spatial analysis method for detecting spatial stratified heterogeneity, is widely used for factor analysis. The Geodetector includes the following four detectors: (1) Differentiation and risk factor detection, the detection of the spatial differentiation of Y, and the extent to which the detection of a factor X explains the spatial differentiation of attribute Y. (2) Interaction detection, which identifies the interaction between different risk factors, i.e., assesses whether factors X1 and X2 increase or decrease the explanatory power of the dependent variable Y when they work together, or whether the effects of these factors on Y are independent of each other. (3) Risk zone detection, which is used to determine whether there is a significant difference in the mean value of attributes between the two sub-regions. (4) Ecological detection, which is used to compare whether there is a significant difference in the effects of two factors X1 and X2 on the spatial distribution of attribute Y. This study primarily utilizes the risk factor detector to explore the spatial stratified heterogeneity of the SEECF and to investigate to what extent GDP and ULUC factors explain the spatial stratified heterogeneity of the SEECF. It assessed the degree of spatial stratified heterogeneity by calculating the q-value of the dependent variable (SEECF). Furthermore, by separately calculating and comparing the q-values of individual factors and the q-value after the combination of two factors, it could determine the presence of interaction between the two factors, as well as the strength, direction, linearity, or non-linearity of the interaction [74]. The expression is as follows:

$$q_p = 1 - \frac{\sum_z N_{pz} \sigma_{pz}^2}{N_p \sigma_p^2} \tag{15}$$

In Equation (15), q_p represents the q-value of the factor p; N_p and σ_p respectively represent the number of observations and the total variance of factor p across the entire study area; N_{pz} and σ_{pz} respectively denote the number and total variance of factor p within the z-th sub-area. The q-value ranges from 0 to 1, with a higher value indicating more significant spatial stratified heterogeneity of the SEECF and stronger explanatory power of the factor for the SEECF. Conversely, a lower value suggests less significance and weaker explanatory power.

3. Study Area and Materials

3.1. Study Area

According to the "Analysis of Population Aging Situation in Wuhan in 2018" report released by the Civil Affairs Bureau of Wuhan, by the end of 2018, the total registered population of Wuhan was 8.8373 million, with 1.2425 million people aged 65 and above, accounting for 14.06% of the total population. This marked the first time it has exceeded 14%, indicating that Wuhan has entered a stage of an aged society. Wuhan comprises seven central urban districts, including Jiang'an District, Jianghan District, Qiaokou District, Hanyang District, Wuchang District, Qingshan District, and Hongshan District. The degree of aging in these central urban districts has consistently ranked in the top 10 among the 13 districts. These central urban districts possess advantageous geographical locations, dense elderly populations, developed economies, convenient transportations, abundant elderly care facilities, and diverse ULUC, making them suitable for studying the spatial equilibrium of urban elderly care facility allocation and its associations with the economy. The geographical location of the study area is shown in Figure 2.

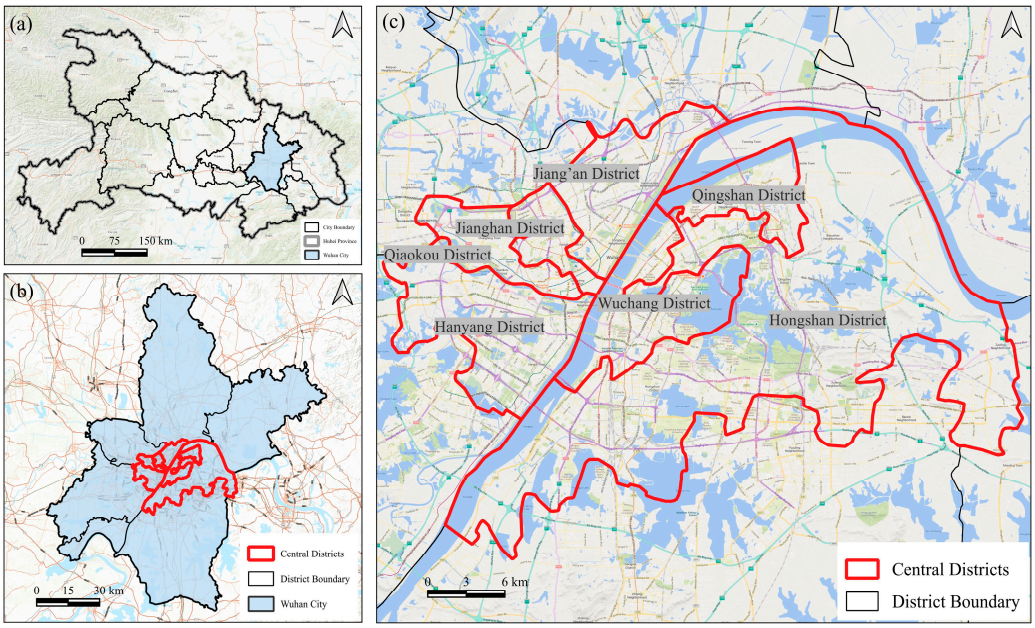

Figure 2. Location of the study area. (**a**) Location of Wuhan in Hubei Province; (**b**) location of central urban area in Wuhan; and (**c**) seven central districts.

3.2. Data Description

3.2.1. Data Sources and Pre-Processing

The data used in this study include population, elderly population (aged 65 and above), points of interest (POI), road network, GDP, primary healthcare facilities, elderly care facilities, and ULUC data. The data information is summarized in Table 2 below:

Regarding POI data, the initial step involved filtering for subcategories under the broad categories of healthcare services and sanatoriums under the category of sports and leisure services. Following this, data cleansing and processing were conducted to obtain datasets of elderly care facilities, with attributes such as the number of beds assigned based on information obtained from the Elderly Care Information Network. Subsequently, subcategories under healthcare services, including clinics and health centers, were selected. Through data cleansing, classification, and processing, primary healthcare facilities were obtained. Which include attributes such as the number of physicians, nurses, and beds. Aging data could be computed based on population and elderly population grid data. ULUC data were converted into raster data, and all raster data were resampled to 100-m

pixel size. The coordinate systems for all data were standardized to the Equal Area Albers projection system (Krasovsky_1940_Albers).

Table 2. Name, source, year, and type of the experimental data.

Name	Source	Year	Type
population	WorldPop (https://hub.worldpop.org, accessed on 23 July 2024)	2010, 2015, 2020	Raster (100 m)
elderly population	WorldPop (https://hub.worldpop.org, accessed on 23 July 2024)	2010, 2015, 2020	Raster (100 m)
POI	Amap (https://ditu.amap.com/, accessed on 23 July 2024)	2010, 2015, 2020	Point
road network	Amap (https://ditu.amap.com/, accessed on 23 July 2024)	2010, 2015, 2020	Line
GDP	https://doi.org/10.6084/m9.figshare.17004523.v1 [75], accessed on 23 July 2024	2010, 2015, 2020	Raster (1000 m)
elderly care facilities	https://www.yanglaocn.com/, accessed on 23 July 2024	2023	Point
ULUC	http://data.ess.tsinghua.edu.cn/ [76], accessed on 23 July 2024	2018	Polygon

3.2.2. Settings of Relevant Parameters

When calculating the SARecs, impedance threshold values of 5, 10, 15, 30, and 60 min were set, respectively, to determine the service areas of elderly care service facilities at different time intervals, as shown in the corresponding initial scoring table in Table 3.

Table 3. Scores of service scope of elderly care service facilities.

Time Period	Score
[0, 5] min	10
(5, 10] min	9
(10, 15] min	8
(15, 30] min	6
(30, 60] min	3
>60 min	0

After comprehensive review and redefinition, the term "elderly care facilities" mentioned in this study included elderly care service facilities and medical facilities. Taking the data of community-based elderly care facilities in the central urban area of Wuhan city as an example for experimentation, elderly care service facilities included nursing homes, homes for the elderly, elderly care homes, senior apartments, daycare centers, elderly daycare centers, and senior activity centers, while medical facilities referred to primary healthcare facilities, including community health service centers, community health service stations, and clinics. According to relevant standards [77], the service radii of elderly care service facilities and primary healthcare facilities are shown in Tables 4 and 5, respectively.

Table 4. Service radii of elderly care service facilities.

Type	Service Radius/m
Homes for the elderly (including social welfare centers, honor homes, and elderly sections in social welfare institutes)	1000
Nursing homes	1000
Elderly care homes	1000
Senior apartments	1000
Elderly daycare centers	500
Daycare centers	500
Senior activity centers	500

Table 5. Service radii of primary healthcare facilities.

Type	Service Radius/m
Community health service centers	1000
Community health service stations	300
Clinics	500

4. Results

In empirical research, we first computed the SEECF for 2010, 2015, and 2020 based on the model constructed in this study. We compared our approach with the classical accessibility assessment method, evaluating the sensitivity to spatiotemporal dynamics using three indicators, i.e., standard deviation, q-value of Geodetector, and the number of significant regions detected by local spatial autocorrelation. Furthermore, employing a panel threshold model, we identified the phased influence patterns of population aging, SEECF, and economic development. Lastly, utilizing factor detection of Geodetector along with bivariate spatial autocorrelation analysis, we investigated the spatial associations among SEECF, economic development, and ULUC.

4.1. SEM-HSTS

The spatial equilibrium of elderly care facilities (SEECF) is an index to quantify the balance of supply and demand distribution of elderly care facilities. It is a numeric variable with a value range of [0, 1]. The spatial equilibrium state of elderly care facilities (SESECF) is an index to evaluate the balance of supply and demand distribution of elderly care facilities, which is a text variable, and its correspondence with the SEECF is shown in Table 6 below. The larger the value of the SEECF, the more imbalanced, and the smaller the value of the SEECF, the morebalanced. This indicates that there is a negative correlation between the SEECF and the SESECF.

Table 6. Table of correspondence between SEECF and SESECF.

SEECF	SESECF
[0, 0.2]	well balanced
(0.2, 0.4]	moderately balanced
(0.4, 0.5]	mildly balanced
(0.5, 0.6]	mildly imbalanced
(0.6, 0.8]	moderately imbalanced
[0.8, 1]	severely imbalanced

To further quantitatively compare the spatial sensitivity of the two methods, this study evaluated three indicators, i.e., standard deviation, q-value of Geodetector, and the number of significant clusters in local spatial autocorrelation. These indicators represented three evaluation dimensions. Since the SEECF, obtained through computation, was dimensionless and ranged from [0, 1], normalization of the accessibility results was required for comparison. A higher standard deviation indicates greater dispersion, hence higher spatial sensitivity. The q-value of Geodetector represents spatial stratified heterogeneity, with a range of [0, 1]. Moreover, calculations were made using the Graphical detector tool in the QGIS software. A higher q-value indicates more pronounced spatial stratified heterogeneity, implying higher spatial sensitivity [78]. The number of significant clusters in local spatial autocorrelation represents local spatial heterogeneity, with a greater quantity indicating more evident local spatial heterogeneity [79], assessed using the Local Moran's I method. Calculations were made using the Univariate Local Moran's I tool in the GeoDa software. In addition to spatial sensitivity, this study also investigated the temporal sensitivity of SEECF and accessibility over different periods using the same indicators. The Differential Local Moran's I method was employed for local spatial autocorrelation.

4.1.1. Distribution of SEECF and Comparison of Spatial Sensitivity between SEECF and Accessibility

The classic accessibility assessment employed the M2SFCA method [72] for computation, contrasting with the spatiotemporal sensitivity of the SEM-HSTS proposed in this study. In ArcGIS, experimental results depicted the SEECF and accessibility distribution maps for the central urban area of Wuhan in 2010, 2015, and 2020 (Figure 3). Figure 3a–c illustrate the SEECF distribution, while Figure 3d–f depict the accessibility distribution. The SEECF was categorized based on computed values, with thresholds delineating balanced from imbalanced conditions. According to international standards, the number of nursing home beds per thousand elderly individuals typically ranges from 40 to 50. The Chinese Ministry of Civil Affairs set a target of 40 beds per thousand elderly individuals in 2020, while the Wuhan city government aimed for five beds per hundred elderly individuals. Building upon the analysis using the M2SFCA method and based on relevant literature [16], we further classified the accessibility of elderly care facilities into six levels based on the number of beds available per 100 elderly individuals, i.e., strong (>5), relatively strong (4–5), slightly strong (3–4), slightly weak (2–3), relatively weak (1–2), and weak (0–1). In traditional evaluation methods [80], the degree of supply–demand matching was directly represented by the accessibility of elderly care facilities, corresponding to SEECF.

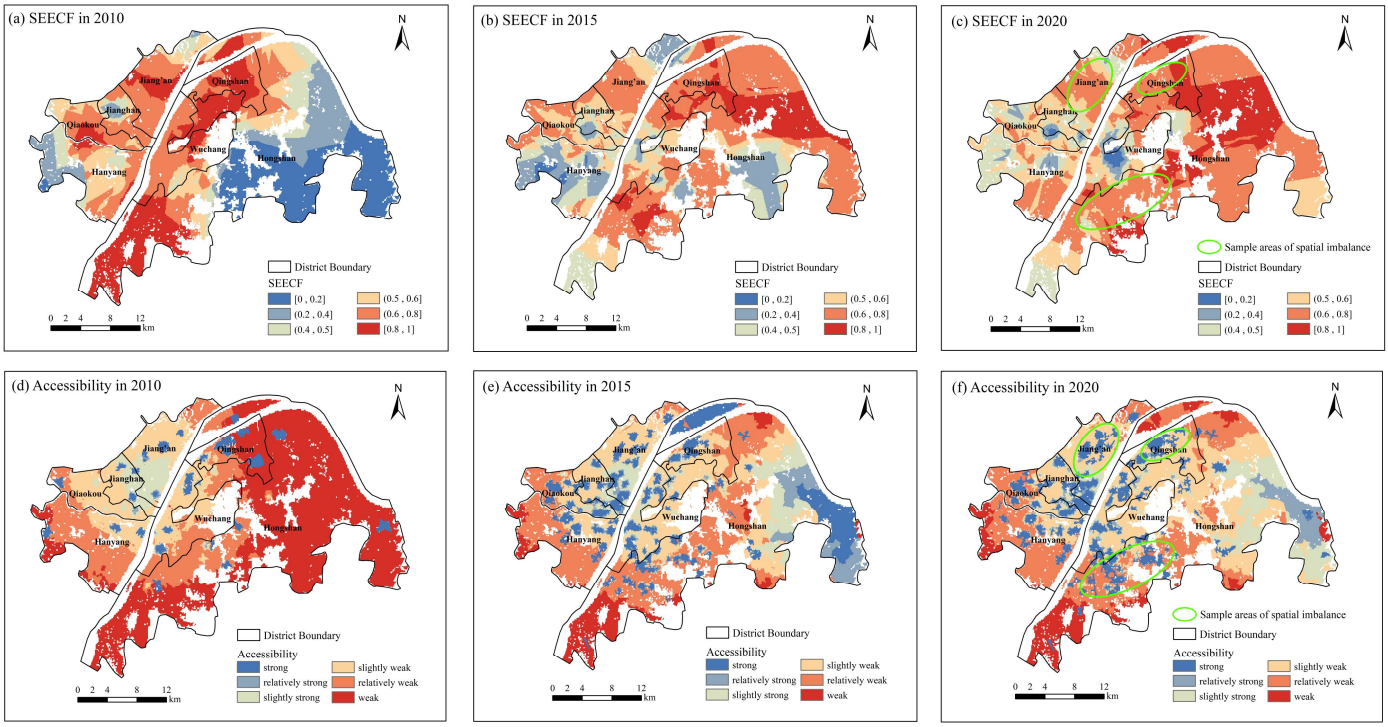

Figure 3. SEECF (spatial equilibrium of elderly care facilities) (**a–c**) and accessibility (**d–f**) distribution maps of elderly care facilities in 2010, 2015, and 2020.

(1) Dissimilarity in the distribution of SEECF.

Figure 3a–c show that over time, the red areas representing spatial imbalance had increased. Overall, the SEECF exhibited a slight tendency towards imbalance. Calculations revealed that the proportion of imbalanced areas had risen from 61.89% to 84.24%. However, significant differences in spatial balance persisted among regions, with distribution remaining uneven. Specifically, in Figure 3a, the core urban areas in 2010 were predominantly imbalanced, primarily due to a supply of elderly care facilities significantly lower than the demand from the population aging, with slightly better spatial balance observed in more peripheral areas. In Figure 3b for 2015, the southwestern and some peripheral areas showed better balance compared to the central core areas, attributed to

the continuous improvement in the quantity and accessibility of facilities alongside the development of elderly care facilities and road networks. However, the growth rate of the elderly population demand in these regions was slower than in the core areas. In Figure 3c for 2020, the balance shifted towards the core areas, mainly due to policy inclinations.

(2) Comparison of spatial sensitivity between SEECF and accessibility.

While the overall findings align with existing research [16,40,42,80,81] and accessibility experiments, there were also divergent results. Taking 2020 as an example, regions marked with green circles in Figure 3c indicated spatial imbalance of SEECF, whereas strong accessibility in Figure 3f implied spatial balance. Further analysis, incorporating elderly care facilities kernel density and elderly population distribution (Figure 4), revealed these areas exhibited an abundance supply of beds but relatively low elderly population numbers, indicative of spatial imbalance resulting from resource inefficiency. Consequently, it preliminarily revealed that the spatial distribution of SEECF proposed in this study was more complex, with significant differences extending beyond the relatively vague phenomena observed at the village and street levels. This advantage stemmed not only from the analysis at the high spatial resolution but also from the careful consideration of the following three factors proposed in this study: SARecs, STSDRecs, and STAms, which accounted for the attenuation of service capacity of elderly care facilities at different scales and the actual needs of the elderly population, thus demonstrating high spatial sensitivity. Based on these findings, precise spatial planning and optimization of existing space for elderly care facilities can be supported with robust geographical information.

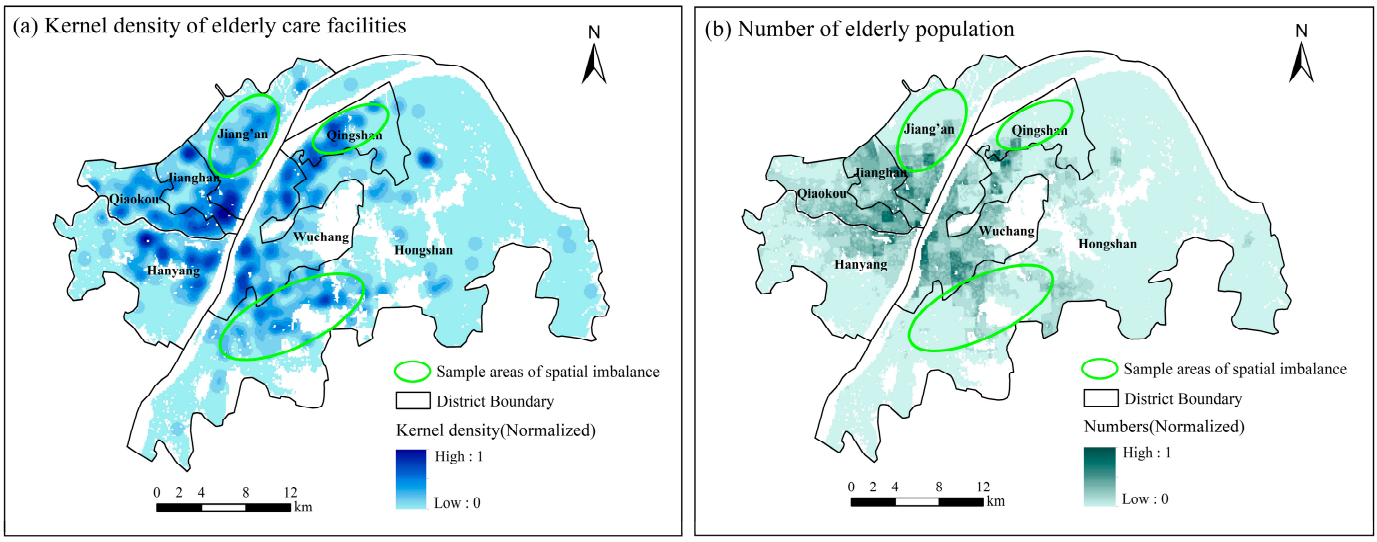

Figure 4. Distribution maps of kernel density of elderly care facilities and number of elderly populations in 2020.

The evaluation of the spatial sensitivity of SEECF and accessibility (Table 7) revealed that the standard deviation of SEECF was greater than that of accessibility each year, indicating higher dispersion compared to accessibility. Additionally, the q-value for SEECF was consistently higher than that for accessibility, signifying more pronounced spatial stratified heterogeneity. With a total grid count of 73,289, the number of significant clusters of SEECF detected by Local Moran's I exceeded that of accessibility, indicating more pronounced local spatial heterogeneity compared to accessibility. Altogether, these findings demonstrated that the SEM-HSTS constructed in this study exhibited higher spatial sensitivity.

Table 7. Results of spatial sensitivity evaluation.

Evaluation Index	2010		2015		2020	
	SEECF	Accessibility	SEECF	Accessibility	SEECF	Accessibility
standard deviation	0.28776	0.03112	0.18348	0.02722	0.15059	0.04008
q-value	0.96679	0.15271	0.93119	0.07929	0.90846	0.12469
the number of significant clusters	45,543	29,680	44,024	27,639	42,788	24,274

4.1.2. Comparison of Temporal Sensitivity between SEECF and Accessibility

The temporal sensitivity evaluation was conducted for the periods 2010 to 2020, 2010 to 2015, and 2015 to 2020 (Table 8). The results indicated that for any given period, the standard deviation of SEECF exceeded that of accessibility, as did the q-value, and the number of significant clusters detected by Differential Local Moran's I was greater than that of accessibility, implying greater temporal heterogeneity compared to accessibility. These findings collectively demonstrated the higher temporal sensitivity of SEM-HSTS. This advantage was primarily attributed to the consideration of changes in service capacity (bed count) and elderly population demand (elderly population) over time within the factors STSDRecs and STAms.

Table 8. Results of temporal sensitivity evaluation.

Evaluation Index	2010–2020		2010–2015		2015–2020	
	SEECF	Accessibility	SEECF	Accessibility	SEECF	Accessibility
standard deviation	0.22820	0.04446	0.20835	0.03446	0.11763	0.03027
q-value	0.97762	0.96697	0.96979	0.96337	0.93602	0.92795
the number of significant clusters	45,237	4290	44,134	5521	37,270	5557

4.2. Analysis of the Associations between SEECF and Economic Development

4.2.1. Influence Relationships between SEECF and Economic Development

(1) Threshold effect test of population aging on GDP.

Experiments were performed in Stata software. Table 9 presents the results of the threshold effect model test for the influence of population aging on GDP. Generally, a p-value < 0.05 indicates the existence of a threshold. The results indicated a single threshold effect test with a p-value of 0.31, suggesting the absence of a threshold effect in the impact of population aging on GDP. The F-value represents the noise level, where a higher value indicates a smaller proportion of noise to the signal. Critical values at 1%, 5%, and 10% indicate the LR statistic accepted at the corresponding levels [49].

Table 9. Threshold effect test of the influence of population aging on GDP.

Threshold Variable: SEECF						
		F-Value	p-Value	Critical Value		
				1%	5%	10%
GDP	Single Threshold	66.57	0.3100	35.6962	24.7155	20.2754

Although there was no threshold effect in the influence of population aging on GDP, implying no significant difference in the effect of population aging on GDP under different SEECF, the results (Table 10) showed negative coefficients for the variables in the right column, indicating an inhibitory effect of population aging on GDP. Additionally, it could be observed that under the backdrop of population aging, the coefficient for population size was 0.8974, while for transportation infrastructure, it was 0.2012. This suggested that the influence of population size on GDP was more potent than transportation infrastructure's.

Table 10. Empirical test of the influence of population aging on GDP.

	Threshold Variable: SEECF
	GDP
Transportation infrastructure	0.2012 (0.0010)
Population size	0.8974 (0.0731)
SEECF $\leq$ 0.6528	−0.1031 (0.1685)
SEECF > 0.6528	−0.2105 (0.1727)
Constant term	−0.5908 (0.3232)
R^2	0.9985
F	345.58

Standard errors are given in parentheses.

(2) Threshold effect test of SEECF on GDP.

Table 11 presents the results of the threshold effect model test for the influence of the SEECF on GDP. The results indicated a single threshold effect test with a *p*-value of 0.0133 and a double threshold effect test with a *p*-value of 0.06, suggesting that the influence of SEECF on GDP existed only as a single threshold effect.

Table 11. Threshold effect test of the influence of SEECF on GDP.

Threshold Variable: Population Aging						
		F-Value	***p*-Value**	**Critical Value**		
				1%	**5%**	**10%**
GDP	Single Threshold	35.11	0.0133	35.2553	29.3000	23.7466
GDP	Double Threshold	25.61	0.0600	32.4780	26.1512	23.0487

Table 12 displays the effect of the SEECF on GDP, with population aging as the threshold variable, where the coefficients are listed in the right column. When the degree of population aging was $\leq$0.0637 (indicating a pre-aging society), the SEECF positively affected GDP, with a coefficient of 0.0247. As the SEECF and the spatial equilibrium state of elderly care facilities (SESECF) are inversely related, SESECF exerted an inhibitory effect on GDP, with a more substantial inhibitory effect as it approached spatial balance. Conversely, when the degree of population aging was >0.0637 (approaching an aging society), the SEECF exerted an inhibitory effect on GDP, with a coefficient of −0.0079. In this scenario, the SESECF promoted GDP, with a more substantial promotional effect as it tends towards spatial balance. The panel threshold model utilized time-series data from 2010 to 2020, enabling the capture of detailed effects over a comprehensive period due to the high temporal sensitivity of SEM-HSTS. These conclusions not only revealed the relationships between the SEECF and GDP but also demonstrated the staged influence patterns under different stages of aging, providing insights for the planning of elderly care facilities considering economic development prerequisites and population aging background. Additionally, it was observed that under the backdrop of SEECF, the coefficient for population size was 0.9127, while for transportation infrastructure, it was 0.1973, indicating that the influence of population size on GDP consistently outweighed that of transportation infrastructure.

Table 12. Empirical test of the influence of SEECF on GDP.

	Threshold Variable: Population Aging
	GDP
Transportation infrastructure	0.1973 (0.0091)
Population size	0.9127 (0.0391)
Population aging $\leq$ 0.0637	0.0247 (0.0134)

Table 12. *Cont.*

	Threshold Variable: Population Aging
	GDP
Population aging > 0.0637	−0.0079 (0.0103)
Constant term	−0.6521 (0.1676)
R^2	0.9986
F	372.80

Standard errors are given in parentheses.

4.2.2. Spatial Associations between SEECF and Economic Development

Following the identification of the phased influence relationships between the SEECF and economic development, this study explored their spatial associations. Initially, based on the bivariate spatial autocorrelation analysis method, an analysis of the SEECF and GDP in the central urban area of Wuhan in 2020 was conducted. Experiments were performed in GeoDa software. The global spatial autocorrelation analysis yielded a Moran's I value of −0.323 with a *p*-value of 0.001. The distribution of points along the horizontal and vertical axes was relatively uniform, indicating a significant negative association between the SEECF and GDP in the central urban area of Wuhan in 2020 within a 99% confidence interval. The results also highlighted the importance of investigating the spatial associations between the two variables. Local Spatial Autocorrelation Analysis results in obtaining a BiLISA cluster map (Figure 5). LISA (Local Indicators of Spatial Association) is a method for spatial data analysis to identify spatial cluster patterns. Based on the similarity of data in geographic space, it calculates the local spatial correlation index of each region so as to judge the local spatial autocorrelation. Figure 5 revealed significant "high-high" clustering, indicating a correlation between high GDP and spatial imbalance in some core areas and transitional zones, accounting for 13.93% of the total. Conversely, "low-low" clustering, denoting a correlation between low GDP and spatial balance, was observed in peripheral areas, representing 4.91% of the total. Additionally, "high-low" clustering, indicating a correlation between high GDP and spatial balance, was prevalent in most areas of the core region, accounting for 21.79% of the total. Furthermore, "low-high" clustering, indicative of a correlation between low GDP and spatial imbalance, was observed in peripheral areas and some transitional zones, representing 17.57% of the total. These phenomena preliminarily reflected the complexity of the spatial correlations between the SEECF and GDP. The areas with high GDP and spatial balance were primarily concentrated in the core region, followed by areas with low GDP and spatial imbalance, showing an uneven distribution. This conclusion confirmed the previously mentioned influence relationships and demonstrated its specific spatial distribution. It was the high spatial sensitivity of SEM-HSTS that enabled the precise identification of the differential distribution associated with GDP. Based on the spatial correlations conclusions, GDP development can be promoted by improving the SESECF in regions.

After the previous analysis, it can be seen that there are phased hierarchical impact relationships and spatial correlation differences between economic development and SEECF. At present, many studies have explored and found that there is a significant spatial association between GDP and different ULUC, so ULUC are likely to affect the spatial allocation of elderly care facilities. In this study, Geodetector was used to study the relative effects of ULUC, GDP, and the interaction between the two on the SESECF. The temporal changes are depicted in Figure 6. It could be observed that over time, and with changes in the SESECF, the influence of GDP on the SESECF was more significant than that of ULUC. Additionally, the combined interaction of ULUC and GDP had a more substantial influence on the SESECF than any single factor alone. This underscored the necessity of considering ULUC when exploring the spatial associations between the SEECF and economic development.

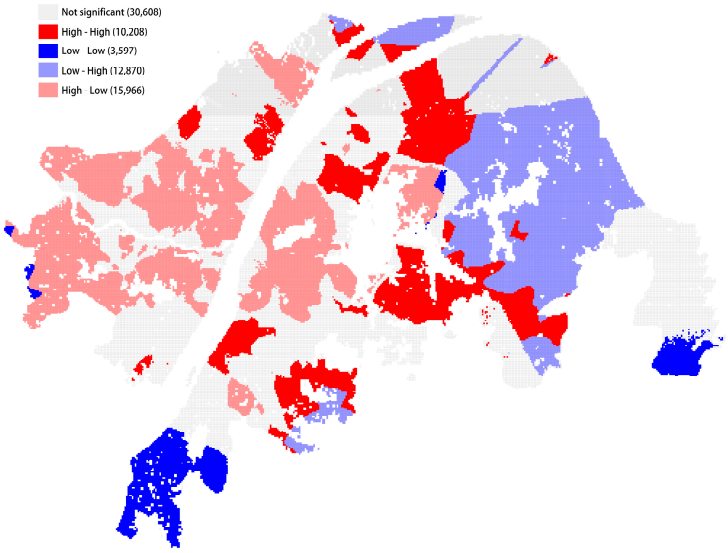

Figure 5. BiLISA cluster map of SEECF and GDP in 2020.

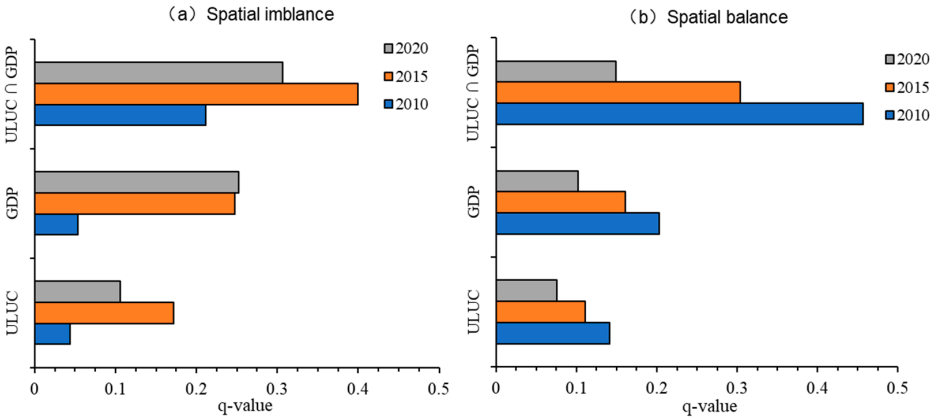

Figure 6. The relative influences of ULUC (urban land use categories), GDP, and their interaction on SESECF (spatial equilibrium state of elderly care facilities). (**a**) The relative influences in spatial imbalance regions; (**b**) the relative influences in spatial balance regions.

In addition, risk area detection, risk factor detection, and ecological detection all indicated significant differences in the influence of GDP versus ULUC on the SEECF, with the former exhibiting a more decisive influence. We further explored the spatial associations in 2020. The spatial distribution maps of SEECF, GDP, and ULUC in the central urban area of Wuhan in 2020 are depicted in Figure 7.

Figure 7c showed that ULUC were diverse and spatially unevenly distributed, with variations in land area. Therefore, the high spatial sensitivity of the SEM-HSTS provided a superior and essential prerequisite for investigating the spatial associations under different ULUC, enabling precise and distinct conclusions. Statistical analysis of SEECF and GDP by ULUC yields Table 13 and Figure 8. Analyzing in conjunction with Figure 7, it was evident that the type with the lowest average value of SEECF, indicating the most balanced, was transportation stations. Simultaneously, this type exhibited the highest average GDP, corresponding to the phenomenon of spatial balance in the core areas correlated with high GDP as mentioned earlier. Similar patterns were observed for business office type, commercial service type, and sport and cultural type. Conversely, the urban land type with the highest average value of SEECF, indicating the most imbalanced, was the airport facility type. Additionally, this type showed the lowest average GDP, corresponding to the phenomenon of spatial imbalance in the peripheral areas with low GDP correlation as mentioned earlier. Similar patterns were observed for medical type, administrative type,

and park and green type. Industrial types near the Qingshan district exhibited spatial imbalance correlated with high GDP, while those near Hanyang district exhibited spatial balance correlated with low GDP. Residential type in the Jiang'an district exhibited spatial imbalance correlated with high GDP, whereas most residential type in other areas exhibited spatial balance correlated with low GDP. Educational type showed no significant correlation between SEECF and GDP. The maximum difference in average values of SEECF among all ULUC was approximately 0.15, with all being in a state of imbalance, indicating an insignificant difference. This also indirectly reflected that the influence of ULUC on SEECF was smaller than that of GDP.

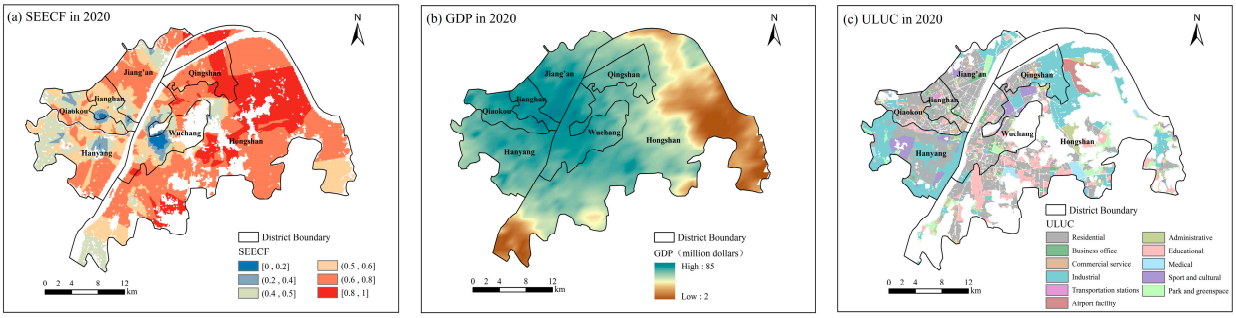

Figure 7. Distribution maps of SEECF, GDP, and ULUC in 2020.

Table 13. Statistical table of SEECF, GDP, and ULUC.

ULUC	Average of SEECF	Average of GDP
Residential	0.648614	53.132159
Business office	0.606417	65.587837
Commercial service	0.527255	61.842093
Industrial	0.595075	44.633519
Transportation stations	0.519569	66.422399
Airport facility	0.762188	25.951213
Administrative	0.746214	38.308079
Educational	0.695867	47.545746
Medical	0.681549	42.278336
Sport and cultural	0.534834	55.892979
Park and greenspace	0.677570	39.862133

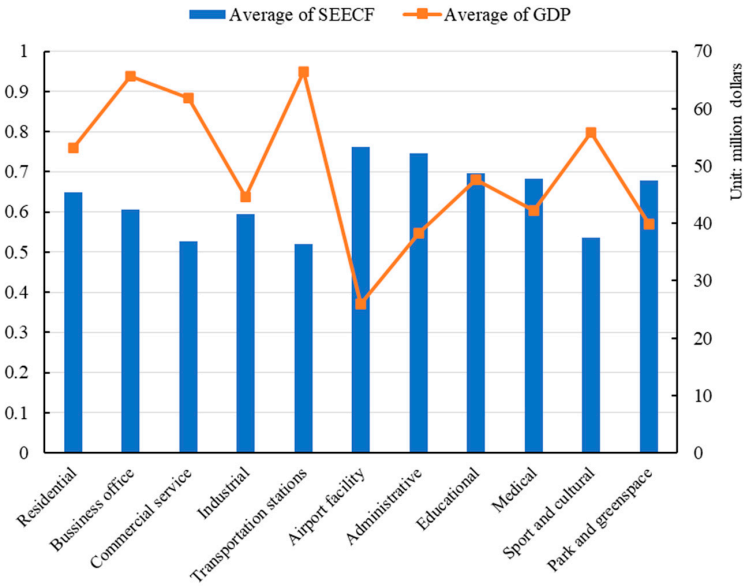

Figure 8. Statistical chart of SEECF, GDP, and ULUC.

5. Discussion

5.1. Study of the SEM-HSTS

In summary, the core areas of the central urban region exhibited a better spatial equilibrium state of elderly care facilities (SESECF), while the peripheral areas showed poorer SESECF. The core areas serve as the leading economic zones in Wuhan, whereas the peripheries are relatively underdeveloped. This indicates that the economic development of a region has a certain degree of influence on the spatial equilibrium state of elderly care facilities (SEECF), consistent with findings from other studies [16]. In the central urban districts of Wuhan, there was a trend towards spatial imbalance in elderly care facilities, accompanied by an uneven development of elderly care services, leading to significant regional disparities and an overall poor SESECF. The spatial equilibrium model of elderly care facilities with high spatiotemporal sensitivity (SEM-HSTS) developed in this study not only demonstrated greater spatiotemporal sensitivity compared to the accessibility method but also identified instances of resource wastage that the latter failed to detect, enabling a more nuanced analysis. Government authorities should intervene with substantive measures tailored to the specific realities, such as regulating existing facility stocks and adjusting the distribution of distribution structures, to reduce disparities and improve resource utilization efficiency.

By observing the three factors (SARecs, STSDRecs, and STAms) and the three indicators (standard deviation, q-value of the Geodetector, and the number of significant clusters in spatial autocorrelation) to evaluate the spatiotemporal sensitivity of the model proposed in this study, we can know where the problems are. Further corrections are made to achieve spatial balance.

5.2. Analysis of the Associations between SEECF and Economic Development

5.2.1. Influence Relationships among SEECF, Population Aging, and GDP

Utilizing the high temporal sensitivity of SEM-HSTS, this study explored the relationships between the SEECF, population aging, and GDP based on panel threshold models. The results indicated that population aging had a restraining effect on GDP. As the population ages, government expenditures on elderly care increase, including pensions, retirement benefits, and healthcare for the elderly. According to the life-cycle consumption theory [82], savings accumulated earlier in life are consumed, leading to greater consumption as the population ages, potentially stimulating GDP growth to a certain extent. However, population aging may exacerbate labor shortages and reduce innovation, thereby lowering societal labor productivity [83–85]. Furthermore, deepening population aging may lead to higher income distribution, reducing the proportion of economic output available for productive investment, thus hindering capital accumulation and lowering the potential economic output level [86,87].

Additionally, it was found that before entering an aging society, the effect of the elderly population size had not yet expanded. At this stage, the SESECF exhibited a restraining effect on GDP; however, upon entering an aging society, as the aging process deepens, although the scale of labor supply decreases and the burden of supporting the elderly increases, the SESECF also improved significantly. Moreover, as it tends toward spatial balance, the demands of the elderly are met while elderly care resources are fully utilized. This benefits the development of the elderly care industry and enhances the ability to attract labor, thereby contributing to GDP growth.

5.2.2. Spatial Associations among GDP, ULUC, and SEECF

Utilizing the high spatial sensitivity of SEM-HSTS, this study explored the spatial associations among GDP, urban land use categories (ULUC), and SEECF. It revealed that the combined interaction effect of ULUC and GDP on SEECF was stronger than any individual factor. Moreover, the influence of GDP on the SEECF was significantly greater than ULUC. This conclusion reaffirms the notion that regional economic development has a significant influence on SEECF, surpassing that of urban functional structure. Further exploration of

the spatial associations among the three variables yielded rich insights, from which several recommendations for the planning of elderly care facilities in the central urban area of Wuhan can be derived as follows:

(1) Poor SESECF was observed in medical and administrative land use types, necessitating measures such as the addition of elderly care facilities and adjustment of distribution structures to enhance SESECF.
(2) Favorable SESECF was observed in commercial service, transportation stations, business offices, and sport and cultural land use types. For the minority of areas experiencing spatial imbalance, improvement can be achieved by adjusting the stock of elderly care facilities, potentially leading to positive effects on GDP.
(3) Residential, industrial, and educational land use types exhibited varied SESECF, requiring improvement strategies tailored to specific distribution patterns, possibly through a combination of both methods.

5.3. Limitations

The future development of urban elderly care facilities should align to achieve refined urban management and fully consider the elderly's preferences for care and medical services. Although this study conducted experiments at a finer grid scale and proposed three factors for constructing the spatial equilibrium model of elderly care facilities, which better reflected the dual perspectives of supply and demand compared to the accessibility method and exhibited greater spatiotemporal sensitivity, the planning recommendations drawn are somewhat limited and biased due to data constraints, as experiments were only conducted on community-based elderly care facilities in the central urban area of Wuhan. When this study explored the impact of GDP and ULUC on the SEECF, it only analyzed how the combined effect of the two affected the SEECF and did not analyze their individual effects. Future research can consider using more rigorous and scientific influencing factor analysis methods to explore the individual and combined effects of GDP and ULUC on the SEECF. It can also look for other relevant influencing factors for analysis and further find the specific impact mechanisms or pathways of each factor on the elderly care facilities. At the same time, it is also necessary to explore the causal relationship between various factors and the SEECF in the next step of work so as to obtain a more comprehensive understanding and lay a solid foundation for the development of practical work. In future work, we can set key parameters in site selection analysis or facility optimization analysis based on the spatial equilibrium model of elderly care facilities proposed in this study and the analysis of the correlation between the SEECF and economic development under the background of population aging, and enhance the existing models so as to provide a more scientific reference for the comprehensive optimization of urban elderly care services and facility planning layout.

6. Conclusions

This study proposes to construct two types of factors, namely the spatial accessibility rate of elderly care services (SARecs) and the spatiotemporal supply–demand ratio for elderly care services (STSDRecs). It further utilizes the modified two-step floating catchment area (M2SFCA) method to obtain the factor of the spatiotemporal availability of medical services (STAms). Subsequently, these three types of factors are introduced into a coordination model to construct the spatial equilibrium model of elderly care facilities with high spatiotemporal sensitivity (SEM-HSTS) at a 100-m grid scale. Leveraging the advantages of high temporal sensitivity, the study employs a panel threshold model to explore the phased relationships among population aging, the spatial equilibrium state of elderly care facilities (SEECF), and GDP. Finally, leveraging the advantages of high spatial sensitivity, the study employs Geodetector to investigate the spatial associations between the SEECF, urban land use categories (ULUC), and GDP. The research findings are as follows:

1. Compared to the classical accessibility method, the SEM-HSTS constructed in this study demonstrates higher spatiotemporal heterogeneity, exhibiting enhanced spa-

tiotemporal sensitivity. Consequently, it can identify various spatial imbalance phenomena, such as insufficient supply and resource wastage. Over time, the overall SEECF in the central urban area of Wuhan shows a weak tendency towards imbalance, with the proportion of imbalanced areas increasing from 61.89% to 84.24%. However, significant differences in SEECF between regions persist, maintaining an uneven distribution. Based on these findings, robust references are provided for more precise spatial planning and optimization of existing spaces for elderly care facilities.

2. The high temporal sensitivity of SEM-HSTS allows the model to capture detailed effects over extended periods, thus obtaining precise threshold values and degrees of influence. Population aging exhibits a suppressive effect on GDP. Before and after entering an aging society, the spatial equilibrium state of elderly care facilities (SESECF) respectively exhibits suppressive and promotional effects on GDP, with a stronger influence as it tends towards spatial balance. The high spatial sensitivity of SEM-HSTS provides a necessary prerequisite for studying the spatial associations under complex and unevenly distributed ULUC, enabling precise and evident conclusions. The influence of GDP on the SESECF outweighs that of ULUC, while the combined interaction of ULUC and GDP has a more substantial influence on the SESECF than any single factor alone. The spatial association between GDP and SESECF under the influence of ULUC is diverse. The types of transportation stations, commercial offices, business offices, commercial services, and sports and cultural facilities showed that the spatial balance of elderly care facilities correlated with high GDP. The airport facility type, medical type, administrative type, and park and green type have the phenomenon of spatial imbalance correlated with low GDP. Educational type showed no significant association between SEECF and GDP. When planning the layout of elderly care facilities, it is feasible to select suitable locations more accurately based on the region's population aging, such as near educational land use type, achieving both spatial balance in elderly care facilities and promoting sustainable economic development objectives. Thereby providing robust geographical and spatial information support for high-quality elderly care services.

Author Contributions: Conceptualization: Hongyan Li, Rui Li, Jing Cai and Shunli Wang; methodology: Hongyan Li, Rui Li and Jing Cai; software: Hongyan Li; validation: Hongyan Li, Rui Li, Jing Cai and Shunli Wang; formal analysis: Hongyan Li and Rui Li; investigation: Hongyan Li; resources: Hongyan Li and Rui Li; data curation: Hongyan Li and Rui Li; writing—original draft preparation: Hongyan Li; writing—review and editing: Hongyan Li, Rui Li, Jing Cai and Shunli Wang; visualization: Hongyan Li; supervision: Rui Li, Jing Cai and Shunli Wang; project administration: Rui Li; funding acquisition: Rui Li. All authors have read and agreed to the published version of the manuscript.

Funding: This work was supported by the National Natural Science Foundation of China (Grant No. U20A2091, 41930107).

Data Availability Statement: The data presented in this study are available upon request from the corresponding author. The data are not publicly available due to restrictions imposed by privacy approval and informed consent agreements regarding study participants.

Acknowledgments: Thanks to Wuhan Geomatic Institute for its support for this work.

Conflicts of Interest: The authors declare no conflicts of interest.

References

1. Cox, P.R. The Aging of Populations and its Economic and Social Implications. *J. R. Stat. Soc. Ser. A* **1958**, *121*, 253–254. [CrossRef]
2. Lin, X.Y. The Resaerch on Spatial Distribution of Elderly Care Facilities in Shanghai—A Case Study of Aged Home and Community Elderly Care Facilities. Master's Thesis, East China Normal University, Shanghai, China, 2016.
3. Wang, X.C.; Xiong, F.; Wang, Z.W.; Chen, S.; Zhang, Z.; Peng, L.N. Planning and layout of facilities for the elders based on POI and machine learning: A case study of Wuhan. *Econ. Geogr.* **2021**, *41*, 49–56. [CrossRef]
4. Ishikawa, N.; Fukushige, M. Dissatisfaction with dwelling environments in an aging society: An empirical analysis of the kanto area in Japan. *Rev. Urban Reg. Dev. Stud.* **2015**, *27*, 149–176. [CrossRef]

5. Singelenberg, J.; Stolarz, H.; McCall, M.E. Integrated service areas: An innovative approach to housing, services and supports for older persons ageing in place. *J. Community Appl. Soc. Psychol.* **2014**, *24*, 69–73. [CrossRef]
6. Yu, S.; Zhu, X.; He, Q. An assessment of urban park access using house-level data in urban China: Through the lens of social equity. *Int. J. Environ. Res. Public Health* **2020**, *17*, 2349. [CrossRef]
7. Lin, W. The relationship between formal and informal care among Chinese older adults: Based on the 2014 CLHLS dataset. *BMC Health Serv. Res.* **2019**, *19*, 1–8. [CrossRef]
8. Jain, S.; Gonski, P.N.; Jarick, J.; Frese, S.; Gerrard, S. Southcare geriatric flying squad: An innovative Australian model providing acute care in residential aged care facilities. *Intern. Med. J.* **2018**, *48*, 88–91. [CrossRef] [PubMed]
9. Wang, F.; He, P.; Yuan, C.; Wang, S. Isolated or integrated? Evaluation of ageing-friendly communities in Old Beijing City based on accessibility, social inclusion and equity. *Indoor Built Environ.* **2020**, *29*, 465–479. [CrossRef]
10. Chen, W.; Cheng, L.; Chen, X.; Chen, J.; Cao, M. Measuring accessibility to health care services for older bus passengers: A finer spatial resolution. *J. Transp. Geogr.* **2021**, *93*, 103068. [CrossRef]
11. Liu, X.C. A Spatial Equilibrium Analysis of Community-Based Elderly Care Facilities in Shijingshan District. Master's Thesis, North China University of Technology, Beijing, China, 2023.
12. Cheng, Y.; Wang, J.; Rosenberg, M.W. Spatial access to residential care resources in Beijing, China. *Int. J. Health Geogr.* **2012**, *11*, 32. [CrossRef]
13. Zhang, H.Y.; Zhang, B.R. Spitial distribution of urban community in- home service facilities for the elderly—A case study of shanghai central area. *Yunnan Geogr. Environ. Res.* **2016**, *28*, 55–59.
14. Chen, R.F. The Research on the Rationality of Spatial Layout of Urban institutional Pension Facilities—Taking Xi'an as an Example. Master's Thesis, Xi'an University of Architecture and Technology, Shanxi, China, 2016.
15. Zhang, Y.; Zhang, M.; Hu, H.; He, X. Spatiotemporal characteristics of the supply and demand coupling coordination of elderly care service resources in China. *Int. J. Environ. Res. Public Health* **2022**, *19*, 10397. [CrossRef] [PubMed]
16. Cai, E.; Liu, Y.; Jing, Y.; Zhang, L.; Li, J.; Yin, C. Assessing spatial accessibility of public and private residential aged care facilities: A case study in Wuhan, Central China. *ISPRS Int. J. Geo-Inf.* **2017**, *6*, 304. [CrossRef]
17. Guagliardo, M.F. Spatial accessibility of primary care: Concepts, methods and challenges. *Int. J. Health Geogr.* **2004**, *3*, 3. [CrossRef]
18. Xia, Y.J.; Deng, S.Y.; Wang, Y. The Rationality of Spatial Allocation of Pension Service Facilities in Hefei City Based on Life Cycle Theory. *Trop. Geogr.* **2021**, *41*, 769–777. [CrossRef]
19. Yang, D.H.; Goerge, R.; Mullner, R. Comparing GIS-based methods of measuring spatial accessibility to health services. *J. Med. Syst.* **2006**, *30*, 23–32. [CrossRef]
20. Xu, X.; Zhao, Y. Spatial distribution pattern and accessibility assessment of pension service facilities in Nanjing: Two-step floating catchment area method based on time cost. *Mod. Urban Res.* **2017**, *2*, 2–11. [CrossRef]
21. Li, H.P.; Liang, Z.H. Research onspatial equilibrium of urban community elderly care facilities and its configuration. *J. Geo-Inf. Sci.* **2021**, *23*, 467–478. [CrossRef]
22. Tao, Z.L.; Cheng, Y.; Dai, T.Q. Measuring spatial accessibility to residential care facilities in Beijing. *Prog. Geogr.* **2014**, *33*, 616–624. [CrossRef]
23. Wang, Y.F.; Zhang, C. GIS and gravity polygon based service area analysis of public facility: Case study of hospitals in Pudong new area. *Econ. Geogr.* **2005**, *25*, 800–803. [CrossRef]
24. Wu, J.J. The Spatial Accessibility Analysis of Rural Medical Facilities Using GIS: A Case Study of Lankao County, Henan Province. Master's Thesis, Henan University, Kaifeng, China, 2008.
25. Spencer, J.; Angeles, G. Kernel density estimation as a technique for assessing availability of health services in Nicaragua. *Health Serv. Outcomes Res. Methodol.* **2007**, *7*, 145–157. [CrossRef]
26. Tsou, K.W.; Hung, Y.T.; Chang, Y.L. An accessibility-based integrated measure of relative spatial equity in urban public facilities. *Cities* **2005**, *22*, 424–435. [CrossRef]
27. Wachs, M.; Kumagai, T.G. Physical accessibility as a social indicator. *Socio-Econ. Plan. Sci.* **1973**, *7*, 437–456. [CrossRef]
28. Bach, L. The problem of aggregation and distance for analyses of accessibility and access opportunity in location-allocation models. *Environ. Plan. A* **1981**, *13*, 955–978. [CrossRef]
29. Pacione, M. Access to urban services—The case of secondary schools in Glasgow. *Scott. Geogr. Mag.* **1989**, *105*, 12–18. [CrossRef]
30. Talen, E.; Anselin, L. Assessing spatial equity: An evaluation of measures of accessibility to public playgrounds. *Environ. Plan. A* **1998**, *30*, 595–613. [CrossRef]
31. Smoyer-Tomic, K.E.; Hewko, J.N.; Hodgson, M.J. Spatial accessibility and equity of playgrounds in Edmonton, Canada. *Can. Geogr./Le Géographe Can.* **2004**, *48*, 287–302. [CrossRef]
32. Launay, L. Methodology for building a geographical accessibility health index throughout metropolitan France. *PLoS ONE* **2019**, *8*, e0221417. [CrossRef]
33. McGrail, M.; Humphreys, J. Measuring spatial accessibility to primary health care services: Utilising dynamic catchment sizes. *Appl. Geogr.* **2014**, *54*, 182–188. [CrossRef]
34. Liu, G.Y.; Li, R.; Xia, J.; Liu, Z.H.; Cai, J.; Wu, H.Y.; Peng, M.J. Dual-environment feature fusion-based method for estimating building-scale population distributions. *Geo-Spat. Inf. Sci.* **2023**, 1–16. [CrossRef]
35. Hu, Q.S.; Li, R.; Wu, H.Y.; Liu, Z.H.; Cai, J. Population Analysis Unit Expression Considering Urban Scene Changes. *Geomat. Inf. Sci. Wuhan Univ.* **2023**. [CrossRef]

36. Wu, H.Y.; Hu, Q.S.; Li, R.; Liu, Z.H. Research progress on spatiotemporal distribution estimation of urban population. *Acta Geod. Cartogr. Sin.* **2022**, *51*, 1827–1847. [CrossRef]
37. Cheng, M.; Huang, W. Measuring the accessibility of residential care facilities in Shanghai based on gaussian two-step floating catchment area method. *J. Fudan Univ. (Nat. Sci.)* **2020**, *59*, 129–136. [CrossRef]
38. Xu, X.M.; Miao, J. Study on the Spatial Distribution of Pension Facilities in Guangzhou. *South Archit.* **2020**, *5*, 98–104. [CrossRef]
39. Luo, W. Using a GIS-based floating catchment method to assess areas with shortage of physicians. *Health Place* **2004**, *10*, 1–11. [CrossRef] [PubMed]
40. Ding, Q.X.; Zhu, X.L.; Luo, J. Analysing spatial accessibility to residential care facilities in Wuhan. *Hum. Geogr.* **2016**, *31*, 36–42. [CrossRef]
41. Zhang, S.; Liu, C.; Wang, H.H. Research on the Equalization of Institutional Pension Facilities Layout in Central Urban Area of Tianjin. *Mod. Urban Res.* **2022**, *1*, 38–44. [CrossRef]
42. He, A.K.; Li, J.S.; Yang, N.N.; Li, L.Z. An Analysis of Temporal and Spatial Pattern of Population aging and Accessibility of Elderly Services in Wuhan. *J. Geomat.* **2020**, *45*, 150–153.
43. Huang, X.R.; Gong, P.X.; White, M. Study on spatial distribution equilibrium of elderly care facilities in downtown Shanghai. *Int. J. Environ. Res. Public Health* **2022**, *19*, 7929. [CrossRef]
44. Chen, X.A.; Xiao, Y.Y. Research on equity of elderly care facility distribution from the perspectiv of community life circles. *Ind. Constr.* **2021**, *51*, 65–74. [CrossRef]
45. Wang, L.; Zhou, K.; Wang, Z. Spatial distribution of community pension facilities from the perspective of health equity: A case study of the central city of shanghai. *Hum. Geogr.* **2021**, *36*, 48–55. [CrossRef]
46. Zhao, X.C.; Qiao, X.C.; Wu, J.L.; Jia, J.; Wang, N.; Wu, C.C. Spatial Analysis on Supply of Home Care Facilities for Aging at Community in Beijing. *Soc. Policy Res.* **2019**, *3*, 39–50. [CrossRef]
47. Luo, W.; Whippo, T. Variable catchment sizes for the two-step floating catchment area (2SFCA) method. *Health Place* **2012**, *18*, 789–795. [CrossRef]
48. Rabiei-Dastjerdi, H.; Matthews, S.A.; Ardalan, A. Measuring spatial accessibility to urban facilities and services in Tehran. *Spat. Demogr.* **2018**, *6*, 17–34. [CrossRef]
49. Li, J.B.; Jiang, Q.B. Population Size, Population aging and Economic Growth. *Popul. J.* **2023**, *45*, 55–66. [CrossRef]
50. Bloom, D.E.; Canning, D.; Fink, G. Implications of population ageing for economic growth. *Oxf. Rev. Econ. Policy* **2010**, *26*, 583–612. [CrossRef]
51. Bloom, D.E.; Finlay, J.E. Demographic change and economic growth in Asia. *Asian Econ. Policy Rev.* **2009**, *4*, 45–64. [CrossRef]
52. Chinn, M.D.; Prasad, E.S. Medium-term determinants of current accounts in industrial and developing countries: An empirical exploration. *J. Int. Econ.* **2003**, *59*, 47–76. [CrossRef]
53. Ingénue, E. Macroeconomic consequences of pension reforms in Europe: An investigation with the INGENUE world model. *CEPREMAP Work. Study* **2001**, *17*, 6–35.
54. Miles, D. Should monetary policy be different in a greyer world? In *Ageing, Financial Markets and Monetary Policy*; Springer: Berlin/Heidelberg, Germany, 2001; pp. 243–276. [CrossRef]
55. Lee, R.; Mason, A.; Miller, T. Life cycle saving and the demographic transition: The case of Taiwan. *Popul. Dev. Rev.* **2000**, *26*, 194–219.
56. Mason, A. Demographic transition and demographic dividends in developed and developing countries. In *United Nations Expert Group Meeting on Social and Economic Implications of Changing Population Age Structures*; Population Division: New York, NY, USA, 2005; Volume 31.
57. Cai, F.; Wang, M. Challenge facing China's economic growth in its aging but not affluent era. *China World Econ.* **2006**, *14*, 20–31. [CrossRef]
58. An, C.B.; Jeon, S.H. Demographic change and economic growth: An inverted-U shape relationship. *Econ. Lett.* **2006**, *92*, 447–454. [CrossRef]
59. Will, M.; Mitra, D. Productivity Growth and Convergence in Agriculture and Manufacturing. *Cent. Int. Econ. Stud. (CIES) Discuss. Study* **1999**, *99*, 18–29. [CrossRef]
60. Ngai, L.R. Barriers and the transition to modern growth. *J. Monet. Econ.* **2004**, *51*, 1353–1383. [CrossRef]
61. Davis, J.C.; Henderson, J.V. Evidence on the political economy of the urbanization process. *J. Urban Econ.* **2003**, *53*, 98–125. [CrossRef]
62. Hansen, G.D.; Prescott, E.C. Malthus to solow. *Am. Econ. Rev.* **2002**, *92*, 1205–1217. [CrossRef]
63. Boucekkine, R.; Croix, D.L.; Licandro, O. Early mortality declines at the dawn of modern growth. *Scand. J. Econ.* **2003**, *105*, 401–418. [CrossRef]
64. Galor, O.; Moav, O. From physical to human capital accumulation: Inequality and the process of development. *Rev. Econ. Stud.* **2004**, *71*, 1001–1026. [CrossRef]
65. Esposito, P.; Patriarca, F.; Perini, L.; Salvati, L. Land degradation, economic growth and structural change: Evidences from Italy. *Environ. Dev. Sustain.* **2016**, *18*, 431–448. [CrossRef]
66. Chumachenko, O.; Openko, I.; Kryvoviaz, Y.; Zhuk, O. Modeling of Indicators of Economic Efficiency of Sectoral Land Use. *Sci. Pap. Ser. E Land Reclam. Earth Obs. Surv. Environ. Eng.* **2022**, *11*, 95–106.

67. Chowdhury, P.; Sikder, M.B. Shoreline dynamics in the reserved region of meghna estuary and its impact on lulc and socio-economic conditions: A case study from nijhum dwip, Bangladesh. *J. Coast. Conserv.* **2024**, *28*, 1–24. [CrossRef]
68. Chen, L.G.; Chen, H.G.; Qu, F.T.; Zhao, C.S. Economic development, industrial restructuring and scale regulation of urban construction land: The case of Ma'anshan City. *Resour. Sci.* **2004**, *26*, 137–144. (In Chinese) [CrossRef]
69. Li, Y.; Li, N. Analysis of influential elements of urban land scale in China. *Urban Plan.* **2006**, *30*, 14–18. [CrossRef]
70. Yu, Y.; Lu, X.H. Contribution Rate of Construction Land to the Secondary and Service Industry Growth: A Case Study of Wuhan City. *Area Res. Dev.* **2010**, *29*, 124–128. [CrossRef]
71. Lou, M.X.; Feng, C.C. Study on the Change of Urban Construction Land and the Different Driving Force in Beijing-Tianjin-and Hebei Region. *Urban Dev. Stud.* **2018**, *25*, 23–28.
72. Delamater, P.L. Spatial accessibility in suboptimally configured health care systems: A modified two-step floating catchment area (M2SFCA) metric. *Health Place* **2013**, *24*, 30–43. [CrossRef]
73. Li, Q.; Su, Y.; Pei, Y. Research on coupling coordination degree model between upstream and downstream enterprises. *Innov. Manag. Ind. Eng.* **2008**, *2*, 172–175. [CrossRef]
74. Wang, J.F.; Xu, C.D. Geodetector:Principle and prospective. *Acta Geogr. Sin.* **2017**, *72*, 116–134. [CrossRef]
75. Chen, J.; Gao, M.; Cheng, S.; Hou, W.; Song, M.; Liu, X.; Liu, Y. Global 1 km × 1 km gridded revised real gross domestic product and electricity consumption during 1992–2019 based on calibrated nighttime light data. *Sci. Data* **2022**, *9*, 202. [CrossRef]
76. Gong, P.; Chen, B.; Li, X.; Liu, H.; Wang, J.; Bai, Y.; Xu, B. Mapping essential urban land use categories in China (EULUC-China): Preliminary results for 2018. *Sci. Bull.* **2020**, *65*, 182–187. [CrossRef]
77. Ministry of Housing and Urban-Rural Development of the People's Republic of China. Announcement of the Ministry of Housing and Urban-Rural Development on the modified revision of the national standard "Code for planning of city and town facilities for the aged" No. 334 of 2018. *Eng. Constr. Stand.* **2019**, *2*, 38–39. [CrossRef]
78. Wang, J.F.; Li, X.H.; Christakos, G.; Liao, Y.L.; Zhang, T.; Gu, X.; Zheng, X.Y. Geographical detectors-based health risk assessment and its application in the neural tube defects study of the Heshun Region, China. *Int. J. Geogr. Inf. Sci.* **2010**, *24*, 107–127. [CrossRef]
79. Anselin, L. Local indicators of spatial association—LISA. *Geogr. Anal.* **1995**, *27*, 93–115. [CrossRef]
80. Peng, J.D.; Xing, L.; Yang, H. Research on planning and layout of elderly care service facilities based on supply-demand matching. *J. Geo-Inf. Sci.* **2022**, *24*, 1349–1362. [CrossRef]
81. Xiao, Y.H.; Wang, H.X.; Zhan, Q.M. Evaluation of Walking Accessibility to Community Health Care from Life Circle Perspective—Taking the Main Urban Area of Wuhan. *J. Geomat.* **2023**, *48*, 121–126. [CrossRef]
82. Auerbach, A.J.; Kotlikoff, L.J. Evaluating fiscal policy with a dynamic simulation model. *Am. Econ. Rev.* **1987**, *77*, 49–55.
83. Davis, C.; Hashimoto, K.I.; Tabata, K. Demographic structure, knowledge diffusion, and endogenous productivity growth. *J. Macroecon.* **2022**, *71*, 103396. [CrossRef]
84. Gordon, R.J. *The Rise and Fall of American Growth: The U.S. Standard of Living since the Civil War*; Princeton University Press: Princeton, NJ, USA, 2017. [CrossRef]
85. Kitao, S.; Mikoshiba, M. Females, the elderly, and also males: Demographic aging and macroeconomy in Japan. *J. Jpn. Int. Econ.* **2020**, *56*, 101064. [CrossRef]
86. Glomm, G.; Ravikumar, B. Productive government expenditures and long-run growth. *J. Econ. Dyn. Control* **1997**, *21*, 183–204. [CrossRef]
87. Lee, R.; Mason, A. Fertility, human capital, and economic growth over the demographic transition. *Eur. J. Popul.* **2010**, *26*, 159. [CrossRef]